

Palladium(II) and Palladium(II)–Platinum(II) Mixed Metal Complexes with Mercapto-1,3,4-thiadiazolate

Hidenori Tannai, Kiyoshi Tsuge,* and Yoichi Sasaki*

Division of Chemistry, Graduate School of Science, Hokkaido University, Sapporo 060-0810

Received February 24, 2006; E-mail: tsuge@sci.hokudai.ac.jp

Mononuclear and dinuclear Pd(II) complexes with mercapto-1,3,4-thiadiazolate were prepared by reacting [Pd(OH)(terpy)](PF_6) with 2-amino-5-mercapto-1,3,4-thiadiazole (Hamct) and 2,5-dimercapto-1,3,4-thiadiazole (H_2dmct). The reaction of [Pd(OH)(terpy)](PF_6) and [Pt(Hdmct)(terpy)](PF_6) resulted in the formation of the Pd(II)–Pt(II) heterometallic complex [{Pd(terpy)}(μ-dmct-*S*,*S*′){Pt(terpy)}](PF_6)$_2$, which showed that dmct^{2-} can be utilized to prepare rationally heterometallic systems. Crystal structure analysis of the complexes showed that the ligands coordinate to the Pd(II) and Pt(II) centers by their mercapto groups in a κ^1S coordination mode. The electronic spectra, redox properties, and molecular orbitals of the palladium complexes have been compared to those of Pt(II) congeners that we reported previously. The properties of a Pd(II)–Pt(II) mixed metal complex were elucidated based on the properties of each metal center.

N-Heteroaromatic compounds with one or two exocyclic thiol groups are useful polydentate ligands that utilize exocyclic sulfur atoms as well as the endocyclic nitrogen atoms for coordination to afford a variety of transition-metal complexes.[1] 2,5-Dimercapto-1,3,4-thiadiazole (H_2dmct) is particularly interesting because with its five donor atoms, it can potentially bind to metal atoms in a variety of coordination modes (Scheme 1).

Three coordination modes for $H_n$dmct$^{(2-n)-}$ have been found by X-ray structural analyses: (i) monodentate coordination of external thiolato sulfur atoms in [Ru(CO)(PPh_3)$_2$(Hdmct-*S*)(Hdmct-*S*,*N*)],[2] (ii) bridging through two external thiolato sulfur atoms in [{Hg(CH_3)}$_2$(μ-dmct-*S*,*S*′)],[3] [{Au(CN^{t}Bu)}$_2$(μ-dmct-*S*,*S*′)],[4] [{Au(PR_3)$_2$}(μ-dmct-*S*,*S*′)] (R_3: Ph_3, Ph_2Py, and Me_3),[5] and [{Au(Ph_2P-E-PPh_2)}$_2$(μ-dmct-*S*,*S*′)] (E: $(CH_2)_6$, $(C_5H_4)Fe(C_5H_4)$, and $CH_2C_6H_4CH_2$),[5] (iii) *N*,*S*-chelate mode in [{Tl(CH_3)$_2$}$_2$(μ-dmct-*N*,*S*)],[6] [{Sn(^{n}Bu)$_2$(μ-dmct-*N*,*N*′,*S*,*S*′)}$_5$],[7] and [Ru(CO)(PPh_3)$_2$(Hdmct-*S*)(Hdmct-*S*,*N*)].[2] In the extended structures, thiolato sulfur atoms further act as a bridge.

We have recently prepared new discrete $H_n$dmct$^{(2-n)-}$ complexes [{Pt(terpy)}(Hdmct-*S*)](PF_6),[8] [{Pt(terpy)}$_2$(μ-dmct-*S*,*S*′)](PF_6)$_2$,[8] and [{Ru(bpy)(terpy)}$_2$(μ-dmct-*S*,*S*′)](PF_6)$_2$.[9] The Pt(II) complex [{Pt(terpy)}(mcmt-*S*)](PF_6)[8] has also been prepared with a related ligand, 2-mercapto-5-methyl-1,3,4-thiadiazolato (mcmt$^-$). In these complexes, the $H_n$dmct$^{(2-n)-}$ ligand uses the thiolato sulfur atoms in either a monodentate or a dithiolato-*S*,*S*′ bridged coordination mode. Precursor complexes with only one coordination site available for H_2dmct or Hmcmt ligand, such as [Pt^{II}(OH)(terpy)]$^+$ and [Ru^{II}(bpy)(terpy)(H_2O)]$^{2+}$, have been used for the preparation of discrete complexes with these ligands.

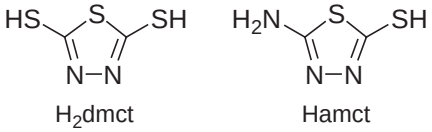

Scheme 1. H_2dmct and Hamct.

Complexes with ratios of $H_n$dmct$^{(2-n)-}$:Pt(II) of 1:1 and 1:2 complexes were selectively obtained by controlling the ratio of reactants. The 1:2 complex was also prepared by the reaction of a second metal complex with the 1:1 complex.[8]

Another important aspect of the dinuclear complex is the redox interaction through the bridging dmct^{2-} ligand featured by the mixed-valence state. For the dinuclear ruthenium complex [{Ru(bpy)(terpy)}$_2$(μ-dmct)]$^{2+}$, the Ru(II)–Ru(III) mixed-valence state was observed during oxidation. The splitting of the oxidation wave into waves corresponding to the Ru_2(II,II)/(II,III) and Ru_2(II,III)/(III,III) couples indicates that there is electronic communication between the two Ru centers through the bridging dmct^{2-}.[9] Upon protonation of a nitrogen donor atom of the bridging ligand, the interaction between metal centers disappears. A similar interaction was not observed for the diplatinum complex.

We have extended our work to include a comparatively labile Pd(II) center by using [Pd(OH)(terpy)]$^+$ as a starting material. In addition to homometallic Pd(II) complexes, a Pd(II)–Pt(II) complex, which is the first heterometallic compound bridged by dmct^{2-}, has been isolated. 2-Amino derivative, amct$^-$ (2-amino-5-mercapto-1,3,4-thiadiazolate) has also been used as a ligand.

Experimental

Materials. The ligands H_2dmct and Hamct were purchased from Tokyo Kasei and Wako chemical, respectively. 2,2′:6′,2″-Terpyridine was purchased from Aldrich. All of the organic solvents, nitric acid, and sodium hydroxide were obtained commercially and used without further purification. The starting complex [Pd(OH)(terpy)](PF_6) was prepared by modifying the published procedure for the corresponding perchlorate salt, i.e., by $NaPF_6$ was used instead of $NaClO_4$.[10] The Pt(II)–Hdmct complex

Published on the web August 7, 2006; doi:10.1246/bcsj.79.1223

[Pt(Hdmct-*S*)(terpy)](PF_6) was prepared as reported previously.[8]

Synthesis. [Pd(amct-*S*)(terpy)](PF_6) ([1](PF_6)): A suspension of [Pd(OH)(terpy)](PF_6) in acetone (50.2 mg, 0.10 mmol, 10 cm^3) was added to a solution of Hamct (13.3 mg, 0.10 mmol) in acetone (20 cm^3) and heptane (1 cm^3). Upon the addition of the [Pd(OH)(terpy)](PF_6) suspension, the mixture turned orange. The solution was then filtered, and slow evaporation of the filtrate at room temperature afforded red crystals of [**1**](PF_6) after two weeks. The crystals were collected by filtration, washed with a small amount of acetone and dried under vacuum. Yield 38 mg, 62%. Anal. Found: C, 32.74; H, 2.21; N, 13.75; S, 10.56%. Calcd for $C_{17}H_{13}F_6N_6PPdS_2$: C, 33.10; H, 2.12; N, 13.62; S, 10.40%; ^{1}H NMR (DMSO-d_6): δ 6.92 (2H, s), 7.91 (2H, t), 8.45 (2H, t), 8.65 (5H, m), 8.92 (2H, d); UV–vis (CH_3CN): λ_{max}/nm (ε/M^{-1} cm^{-1}) 362 (1.02×10^4), 345 (1.13×10^4), 330 (1.03×10^4), 270 (2.89×10^4).

[Pt(amct-*S*)(terpy)](PF_6) ([2](PF_6)): A suspension of [Pt(OH)(terpy)](PF_6) in acetone (59 mg, 0.10 mmol, 10 cm^3) was added to an acetone solution of Hamct (13.4 mg, 0.10 mmol, 70 cm^3) to afford a red-purple solution. Then, the solution was filtered, and slow evaporation of the filtrate at room temperature resulted in the formation of red-purple crystals of [**2**](PF_6) after a few days. The crystals were collected by filtration, washed with small amount of acetone and dried under vacuum (47 mg, 0.067 mmol, 67%). Anal. Found: C, 28.96; H, 1.98; N, 11.86; S, 8.84%. Calcd for $C_{17}H_{13}F_6N_6PPtS_2$: C, 28.94; H, 1.86; N, 11.91; S, 9.09%; ^{1}H NMR (DMSO-d_6): δ 6.82 (2H, s), 7.96 (2H, t), 8.51 (2H, t), 8.70 (5H, m), 9.09 (2H, d); UV–vis (CH_3CN): λ_{max}/nm (ε/M^{-1} cm^{-1}) 492 (8.67×10^2), 344 (1.58×10^4), 329 (1.30×10^4), 280 (3.10×10^4).

[{Pd(terpy)}$_2$(μ-dmct-*S*,*S*′)](PF_6)$_2$ ([3](PF_6)$_2$): An acetonitrile solution of H_2dmct (7.5 mg, 0.05 mmol, 5 cm^3) was added to an acetonitrile solution of [Pd(OH)(terpy)](PF_6) (50.2 mg, 0.1 mmol, 15 cm^3), which afforded an orange solution. The solution was then filtered, and diffusion of diethyl ether into the filtrate resulted in the formation of orange needles of [**3**](PF_6)$_2$·2CH_3CN after 10 d. The crystals were collected by filtration, washed with small amount of diethyl ether and dried under vacuum. The crystal solvent is released from the crystals under reduced pressure. Yield 26 mg, 47%. Anal. Found: C, 34.09; H, 1.99; N, 9.88; S, 8.25%. Calcd for $C_{32}H_{22}F_{12}N_8P_2Pd_2S_3$: C, 34.39; H, 1.98; N, 10.03; S, 8.61%; ^{1}H NMR (DMSO-d_6): δ 7.83 (2H, t), 8.44 (2H, t), 8.66 (5H, m), 8.81 (2H, d); UV–vis (CH_3CN): λ_{max}/nm (ε/M^{-1} cm^{-1}) 362 (1.90×10^4), 345 (2.25×10^4), 329 (2.27×10^4), 268 (5.10×10^4).

[{Pd(terpy)}{Pt(terpy)}(μ-dmct-*S*,*S*′)](PF_6)$_2$ ([4](PF_6)$_2$): An acetonitrile solution of [Pd(terpy)(OH)](PF_6) (25.9 mg, 0.05 mmol, 5 cm^3) was added to an acetonitrile solution of [Pt(terpy)(Hdmct)](PF_6) (36.1 mg, 0.05 mmol, 15 cm^3). Then, the resulting red solution was filtered, and the diffusion of diethyl ether into the filtrate over 10 d afforded red crystals of [**4**](PF_6)$_2$·2CH_3CN. The crystals were collected by filtration, washed with diethyl ether, and dried under vacuum. The crystal solvent is released from the crystals under reduced pressure. Yield 33 mg, 55%. Anal. Found: C, 31.98; H, 2.02; N, 9.53; S, 7.83%. Calcd for $C_{32}H_{22}F_{12}N_8P_2PdPtS_3$: C, 31.87; H, 1.84; N, 9.29; S, 7.98%. ^{1}H NMR (DMSO-d_6): δ 7.85 (4H, m), 8.46 (4H, m), 8.66 (10H, m), 8.79 (2H, s), 9.03 (2H, t); UV–vis (CH_3CN): λ_{max}/nm (ε/M^{-1} cm^{-1}) 481 (1.70×10^3), 361 (1.39×10^4), 344 (2.60×10^4), 328 (2.54×10^4).

X-ray Diffraction Studies. Suitable single crystals of [**1**](PF_6), [**2**](PF_6), [**3**](PF_6)$_2$·2CH_3CN, and [**4**](PF_6)$_2$·2CH_3CN were obtained as described in the preparation section, and were mounted onto a thin glass fiber. Data for [**1**](PF_6), [**2**](PF_6), and [**4**](PF_6)$_2$·2CH_3CN were collected using a Mercury CCD area detector coupled with a Rigaku AFC-8S diffractometer while a Mercury CCD area detector coupled with a Rigaku AFC-7R diffractometer was used for [**3**](PF_6)$_2$·2CH_3CN. Data were collected at -120 °C and the graphite-monochromated Mo Kα radiation was employed. Final cell parameters were determined from least-squares analyses of reflections with $I > 10\sigma(I)$. Space group determinations were made on the basis of systematic absences, a statistical analysis of intensity distribution, and the successful solution and refinement of the structures. Data were collected and processed using Crystal Clear.[11] An empirical absorption correction resulted in acceptable transmission factors. The data were corrected for Lorentz and polarization factors.

All calculations were carried out using a Silicon Graphics O2 computer system and the software package teXsan.[12] The structures were solved by direct methods and expanded using Fourier and difference Fourier techniques. The $dmct^{2-}$ ligands were disordered in the structures of [**3**](PF_6)$_2$·2CH_3CN and [**4**](PF_6)$_2$·2CH_3CN since those ligands were located on inversion centers. When the space group was assumed to be $P1$, the disorder remained, and the R value did not improve. Therefore, the space group of the crystals was determined as $P\bar{1}$. Details of crystal parameters and structure refinement are summarized in Table 1. Selected bond lengths and angles are listed in Table 2. Crystallographic data have been deposited with Cambridge Crystallographic Data Centre: Deposition numbers CCDC 299108–299111. Copies of the data can be obtained free of charge via http://www.ccdc.cam.ac.uk/conts/retrieving.html (or from the Cambridge Crystallographic Data Centre, 12, Union Road, Cambridge, CB2 1EZ, UK; Fax: +44 1223 336033; e-mail: deposit@ccdc.cam.ac.uk).

Computational Methods. Molecular orbital calculations were performed using the Gaussian 03 program[13] at the B3LYP[14] level using a Lanl2DZ[15] basis set. Single-point DFT calculations were carried out for the cation complexes, [Pd(amct)(terpy)]$^+$ and [Pt(amct)(terpy)]$^+$. The structural parameters of the complex cations are taken from the results of X-ray analyses.

Results and Discussion

Syntheses. In our previous report, we showed that the hydroxo complex [Pt(OH)(terpy)]$^+$ is a good starting material for the preparation of $H_n$$dmct^{(2-n)-}$ and $mcmt^-$ complexes of Pt(II).[8] The ligands coordinate to Pt(II) by the external thiolato group. The 1:1 complex [Pt(κ^1-*S*-Hdmct)(terpy)]$^+$ was isolated, from which the 1:2 complex were prepared by reacting with additional [Pt(OH)(terpy)]$^+$. The 1:2 complex was also prepared directly from H_2dmct and [Pt(OH)(terpy)]$^+$ when the reactants are in a 1:2 ratio, respectively.

In this study, a similar approach was used to prepare [Pt(κ^1-*S*-amct)(terpy)](PF_6) ([**2**](PF_6)). The palladium congener [Pd(κ^1-*S*-amct)(terpy)](PF_6) ([**1**](PF_6)) was prepared similarly using [Pd(OH)(terpy)](PF_6). However, the reaction of [Pd(OH)(terpy)]$^+$ with H_2dmct afforded only the dinuclear palladium complex [{Pd(terpy)}$_2$(μ-dmct-*S*,*S*′)](PF_6)$_2$ ([**3**](PF_6)$_2$), which has bridging $dmct^{2-}$ ligand. The 1:1 complex [Pd(Hdmct)(terpy)]$^+$ has not been isolated even when the reactant ratio was 1:1. The substitutionally labile Pd(II) center, in contrast to inert Pt(II) center,[16] may be responsible for the selective formation of the dimer, and it is best to use a 1:2 reactant ratio (H_2dmct/[Pd(OH)(terpy)]$^+$) when preparing [**3**]$^{2+}$.

Table 1. Summary of X-ray Data Collection and Refinement

Compound	[**1**](PF_6)	[**2**](PF_6)	[**3**](PF_6)$_2$·2CH_3CN	[**4**](PF_6)$_2$·2CH_3CN
Formula	$C_{17}H_{13}F_6N_6PPdS_2$	$C_{17}H_{13}F_6N_6PPtS_2$	$C_{36}H_{28}F_{12}N_{10}P_2Pd_2S_3$	$C_{36}H_{28}F_{12}N_{10}P_2PdPtS_3$
Formula weight	616.81	705.50	1199.59	1288.28
Crystal system	triclinic	triclinic	triclinic	triclinic
Space group	$P\bar{1}$	$P\bar{1}$	$P\bar{1}$	$P\bar{1}$
a/Å	6.688(1)	6.718(2)	6.128(2)	6.136(2)
b/Å	9.439(2)	9.413(4)	13.551(4)	13.555(4)
c/Å	16.918(4)	16.932(7)	13.035(4)	13.038(4)
α/°	102.382(3)	102.940(5)	95.684(8)	96.23(1)
β/°	99.778(4)	99.553(5)	82.208(7)	82.15(1)
γ/°	89.880(4)	90.095(5)	101.176(7)	101.42(1)
V/Å^3	1027.4(4)	1028.3(7)	1049.1(5)	1049.3(5)
Z	2	2	1	1
Temp/K	153	153	153	153
ρ_{calcd}/g cm^{-3}	1.602	2.278	1.899	2.039
μ/mm^{-1}	1.259	7.151	1.181	4.068
No. of measured reflns	6582	5678	8654	6313
No. of unique reflns	4150	4009	4633	4265
R_{int}	0.022	0.028	0.019	0.026
No. of reflns ($I > 2\sigma(I)$)	3502	3941	4080	3656
No. of parameters	298	298	307	307
$R1(I > 2\sigma(I))$[a)]	0.0461	0.0286	0.0485	0.0466
$wR2$ (all)[b)]	0.1079	0.0834	0.1236	0.1077
GOF[c)]	1.019	1.040	1.372	1.177

a) $R1 = \Sigma||F_o| - |F_c||/\Sigma|F_o|$. b) $wR2 = \{\Sigma[w(F_o^2 - F_c^2)^2]/\Sigma[w(F_o^2)^2]\}^{1/2}$ with $w = \{\sigma^2(F_o^2) + [x(\max(F_o^2, 0) + 2F_c^2)/3]^2\}^{-1}$. c) GOF $= ((\Sigma w(|F_o| - |F_c|)^2)/(N_o - N_v))^{1/2}$; with N_o = no. of obsd reflns and N_v = no. of parameters.

Complexes [**1**](PF_6) and [**3**](PF_6)$_2$ are the first examples of palladium complexes having mercaptothiadiazolato ligands. The mercaptothiadiazolato ligands are coordinated to palladium centers by the exocyclic sulfur atoms (vide infra). The amino nitrogen does not participate in the coordination. As in the case of the Pt(II) complexes, the hydroxo ligand of $[Pd(OH)(terpy)]^+$ may remove the acidic proton of the mercaptothiadiazoles in the formation of the mercaptothiadiazolato complexes.

The reaction of [Pt(Hdmct)(terpy)](PF_6) and 1 equiv of [Pd(OH)(terpy)](PF_6) afforded the mixed metal complex [**4**](PF_6)$_2$. Complex [**4**](PF_6)$_2$ is the first example of a heterometallic complex with dmct ligand. The result indicates that the mononuclear Hdmct complexes $[Pt^{II}(Hdmct)(terpy)]^+$ and $[Ru^{II}(Hdmct)(bpy)(terpy)]^+$ may be utilized as a building unit for constructing heteronuclear complexes.

Structures. The crystal structures of [**1**](PF_6), [**2**](PF_6), [**3**](PF_6)$_2$·2CH_3CN, and [**4**](PF_6)$_2$·2CH_3CN have been determined by single crystal X-ray analysis. The palladium atom in $[\mathbf{1}]^+$ has a square-planar coordination geometry with the three nitrogen atoms of terpy ligand and the exocyclic sulfur atom of amct$^-$ (Fig. 1a). The bond distances around palladium ion are in the range of those observed in other square-planar Pd(II) complexes.[17] The S1–C1 and N1–C1 distances are 1.747(5) and 1.293(6) Å, respectively, meaning that the coordinated amct$^-$ takes thiolate form.[1,8] The distance between palladium ion and the endocyclic nitrogen atom of amct$^-$ is 3.279(4) Å, which is too long for any interaction between them.

In the crystal of [**1**](PF_6), two complex cations form a pairwise structure via hydrogen bonds between the amine hydrogen and the endocyclic nitrogens (Fig. 1b). The structure is similar to the pairwise structure of $[Pt(Hdmct)(terpy)]^+$, where the hydrogen bonds formed between a thiolate hydrogen atom and a ring nitrogen atom.[8] Hydrogen bonds between coordinated amct ligands have been also reported for the gold complex [Au(amct)(PPh_3)].[18]

The crystal structure of platinum amct complex [**2**](PF_6) was almost identical to that of [**1**](PF_6). The differences in cell constants between [**1**](PF_6) and [**2**](PF_6) are within 0.6% (Table 2), which means that these crystals can be regarded as isomorphous. Indeed, the coordination geometries and the bond distances are almost identical between the two complexes (Fig. 2).

The structure of complex cation $[\mathbf{3}]^{2+}$ is shown in Fig. 3. The crystals of [**3**](PF_6)$_2$ contained two acetonitrile molecules per unit cell; however, those of the Pt analog recrystallized from acetone contained two acetone molecules.[8] The structure of the cation $[\mathbf{3}]^{2+}$ is similar to that of the Pt analog $[\{Pt(terpy)\}_2(dmct)]^{2+}$ in many respects. The complex cation has a crystallographically imposed inversion center on the dmct^{2-} ligand. Two $\{Pd(terpy)\}^{2+}$ units are identical and the thiadiazole ring of dmct^{2-} is disordered in two positions. Although the disorder in the dmct ligand prevents discussion of the S–C and N–C bond distances in dmct^{2-}, the thiol groups of dmct^{2-} should have been deprotonated to afford thiolate moieties, similar to the corresponding platinum complex.[8] The coordination geometry and the bond distances around Pd atom are almost identical to those in [**1**](PF_6).

The structure of $[\mathbf{4}]^{2+}$ is shown in Fig. 4. The crystal of [**4**](PF_6)$_2$·2CH_3CN is isomorphous to that of [**3**](PF_6)$_2$·2CH_3CN (Table 1). Because of the similarity between $\{Pd(terpy)\}^{2+}$ and $\{Pt(terpy)\}^{2+}$ units, the two sites are disordered in struc-

Table 2. Selected Bond Distances (Å) and Angles (°) for [**1**](PF_6), [**2**](PF_6), [**3**](PF_6)$_2$·2CH_3CN, and [**4**](PF_6)$_2$·2CH_3CN

[**1**](PF_6)			
Pd1–S1	2.296(1)	S1–Pd1–N4	97.4(1)
Pd1–N4	2.044(4)	S1–Pd1–N5	177.4(1)
Pd1–N5	1.965(4)	S1–Pd1–N6	101.4(1)
Pd1–N6	2.035(4)	N4–Pd1–N5	81.0(1)
S1–C1	1.747(5)	N4–Pd1–N6	161.1(1)
N1–C1	1.293(6)	N5–Pd1–N6	80.2(2)
N2–C2	1.301(6)	Pd1–S1–C1	103.4(2)
N3–C2	1.351(6)		
[**2**](PF_6)			
Pt1–S1	2.302(1)	S1–Pt1–N4	97.43(10)
Pt1–N4	2.027(3)	S1–Pt1–N5	177.59(10)
Pt1–N5	1.962(3)	S1–Pt1–N6	101.12(10)
Pt1–N6	2.017(3)	N4–Pt1–N5	81.0(1)
S1–C1	1.743(4)	N4–Pt1–N6	161.4(1)
N1–C1	1.289(5)	N5–Pt1–N6	80.5(1)
N2–C2	1.308(5)	Pt1–S1–C1	104.6(1)
N3–C2	1.360(5)		
[**3**](PF_6)$_2$·2CH_3CN			
Pd1–S1	2.306(1)	S1–Pd1–N3	98.4(1)
Pd1–N3	2.029(4)	S1–Pd1–N4	179.3(1)
Pd1–N4	1.970(4)	S1–Pd1–N5	100.0(1)
Pd1–N5	2.034(4)	N3–Pd1–N4	80.9(1)
S1–C1	1.710(8)	N3–Pd1–N5	161.5(1)
		N4–Pd1–N5	80.7(1)
[**4**](PF_6)$_2$·2CH_3CN			
M1–S1	2.317(2)	S1–Pt1–N3	98.1(2)
M1–N3	2.020(6)	S1–Pt1–N4	179.5(2)
M1–N4	1.955(5)	S1–Pt1–N5	99.6(2)
M1–N5	2.024(5)	N3–Pt1–N4	81.4(2)
S1–C1	1.70(1)	N3–Pt1–N5	162.3(2)
		N4–Pt1–N5	80.9(2)

ture of [**4**](PF_6)$_2$·2CH_3CN. A crystallographically imposed inversion center causes disorder in the metal centers and in the thiadiazole ring of $dmct^{2-}$. Although the disorder prevents a detailed discussion of coordination geometries around the palladium and platinum atoms, the bond lengths are comparable to the average values of M–N and M–S distances observed in the two homometal dimers $[\{M(terpy)\}_2(\mu\text{-dmct})]^{2+}$ (M = Pd and Pt).

UV–Vis Absorption Spectra. UV–vis absorption spectra of [**1**](PF_6), [**2**](PF_6), [**3**](PF_6)$_2$, and [**4**](PF_6)$_2$ in CH_3CN are shown in Fig. 5. All of the complexes show similar spectral patterns, i.e., a broad visible band around 500 nm ($\varepsilon \approx 1 \times 10^3\,M^{-1}\,cm^{-1}$), strong structured bands in UV region <350 nm ($\varepsilon \geq 1 \times 10^4\,M^{-1}\,cm^{-1}$), and shoulders in the region of 350–400 nm ($\varepsilon \approx 5 \times 10^3\,M^{-1}\,cm^{-1}$). Based on the spectra of [Pt(Hdmct)(terpy)](PF_6) and [{Pt(terpy)}$_2$(μ-dmct)](PF_6)$_2$,[8] these features may be assigned as S(p) to terpy(π^*) LLCT transition, intra-ligand π–π^* transition of terpy, and the MLCT transition in $\{M(terpy)\}^{2+}$ unit (M = Pd(II) and Pt(II)),

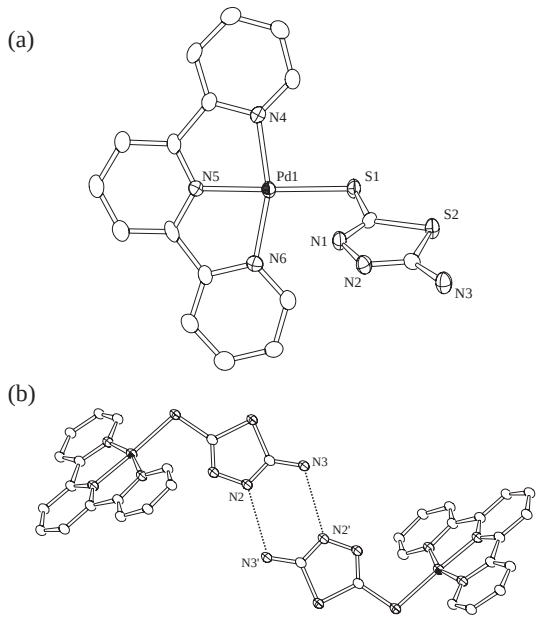

Fig. 1. ORTEP diagrams of the cation complex [**1**]$^+$ (a) and its hydrogen-bonded dimeric structure (b) with 50% thermal ellipsoids. Hydrogen atoms are omitted for clarity.

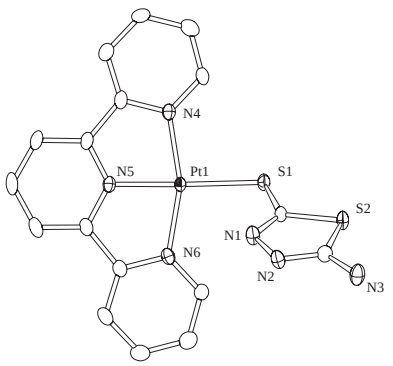

Fig. 2. ORTEP diagram of the cation complex [**2**]$^+$ with 50% thermal ellipsoids. Hydrogen atoms are omitted for clarity.

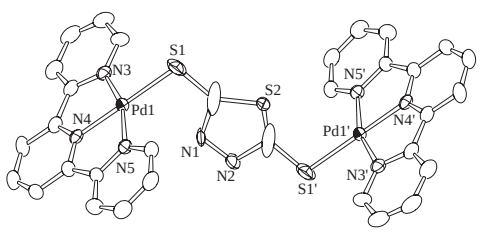

Fig. 3. ORTEP diagram of the cation complex [**3**]$^{2+}$ with 50% thermal ellipsoids. Hydrogen atoms are omitted for clarity. One position of disordered $dmct^{2-}$ is shown.

respectively.[8,19] The differences in the metal ions, Pd(II) or Pt(II), and those in the ligands, $amct^-$, $Hdmct^-$, or $dmct^{2-}$ do not appear to affect the spectral pattern significantly.

The spectrum of the mixed metal complex [**4**](PF_6)$_2$ can be interpreted as the sum of the platinum and palladium complexes, meaning that there is no strong electronic interaction

between the two metal centers bridged by $dmct^{2-}$.

Since *S*-coordinated mercaptothiadiazoles have free nitrogen sites on the ring, the effects of protonation on the spectra was examined by adding TsOH (*p*-toluenesulfonic acid) (Fig. 6). The broad visible band of each complex blue shifted upon addition of TsOH. Subsequent addition of one equivalent of a base, such as NEt_3, caused the initial spectra to reappear. Thus, the spectral changes are due to an acid–base equilibrium. The spectral changes were observed over the addition of five equivalent amount of TsOH suggesting that the protonation is not quantitative with TsOH. The basicity of the free coordination sites may not be sufficiently strong against TsOH in CH_3CN. The blue shift of the visible band on protonation is in good agreement with the assignment of the band as an LLCT band, since the protonation should stabilize the orbitals on the anionic ligand.[9] Although the dinuclear complexes [**3**]$(PF_6)_2$ and [**4**]$(PF_6)_2$ have the isosbestic points during the addition of TsOH, no isosbestic points were observed in case of the amct complexes [**1**](PF_6) and [**2**](PF_6). However, the original spectra reappeared upon the addition of the base. The $amct^-$ ligands in these complexes have a free amine group in addition to the nitrogen sites in the thiadiazole ring. The competitive protonation of these two sites, or the formation of hydrogen-bonded dinuclear complexes, may explain the complicated behavior upon the addition of the acid.

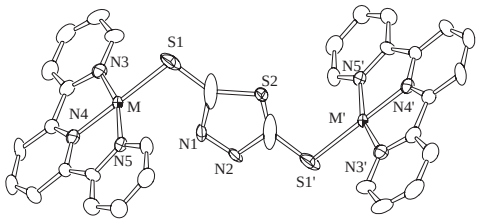

Fig. 4. ORTEP diagram of the cation complex $[\mathbf{4}]^{2+}$ with 50% thermal ellipsoids. Hydrogen atoms are omitted for clarity. Platinum and palladium atoms occupied the M position with the same probability. One position of disordered $dmct^{2-}$ is shown.

Redox Properties. Cyclic voltammograms of [**1**](PF_6), [**2**](PF_6), [**3**]$(PF_6)_2$, and [**4**]$(PF_6)_2$ in DMF are shown in Fig. 7. In the potential region from -1.5 to 1.5 V vs Ag/AgCl, no reversible process was observed except for [**2**](PF_6). The reduction and oxidation processes were observed at potentials less than -0.6 V and greater than 1.0 V, respectively. In the voltammogram of [**2**](PF_6), two redox couples were observed at around -0.7 and -1.3 V, similar to $[Pt(mcmt)(terpy)]^+$, $[Pt(Hdmct)(terpy)]^+$, and $[\{Pt(terpy)\}_2(\mu\text{-dmct})]^{2+}$, and are assigned to the redox processes of the terpy ligand. Only cathodic waves were observed for the palladium complexes for the reduction processes. Since the irreversible cathodic waves for the Pd complexes were observed at almost the same potential to those of Pt analogues, these waves are also assigned to the reduction of the terpy ligand.[8] The oxidation process may be attributed to the oxidation of amino group in case of [**1**](PF_6) and [**2**](PF_6) and to the oxidation of thiolate groups in case of [**3**]$(PF_6)_2$ and [**4**]$(PF_6)_2$. No electronic interaction between the two metal centers was observed for the

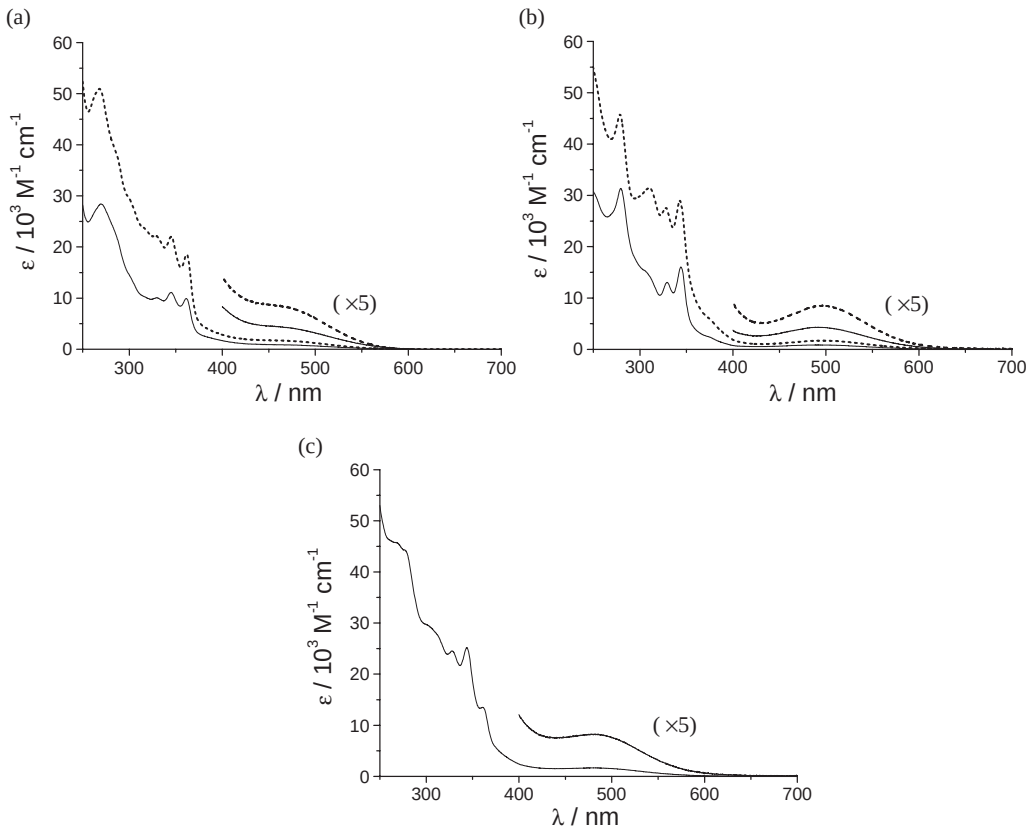

Fig. 5. UV–vis absorption spectra of the palladium (a), platinum (b), and mixed metal (c) complexes in acetonitrile; (a): [**1**](PF_6) (solid line) and [**3**]$(PF_6)_2$ (dotted line), (b): [**2**](PF_6) (solid line) and $[\{Pt(terpy)\}_2(\mu\text{-dmct})](PF_6)_2$ (dotted line), (c): [**4**]$(PF_6)_2$.

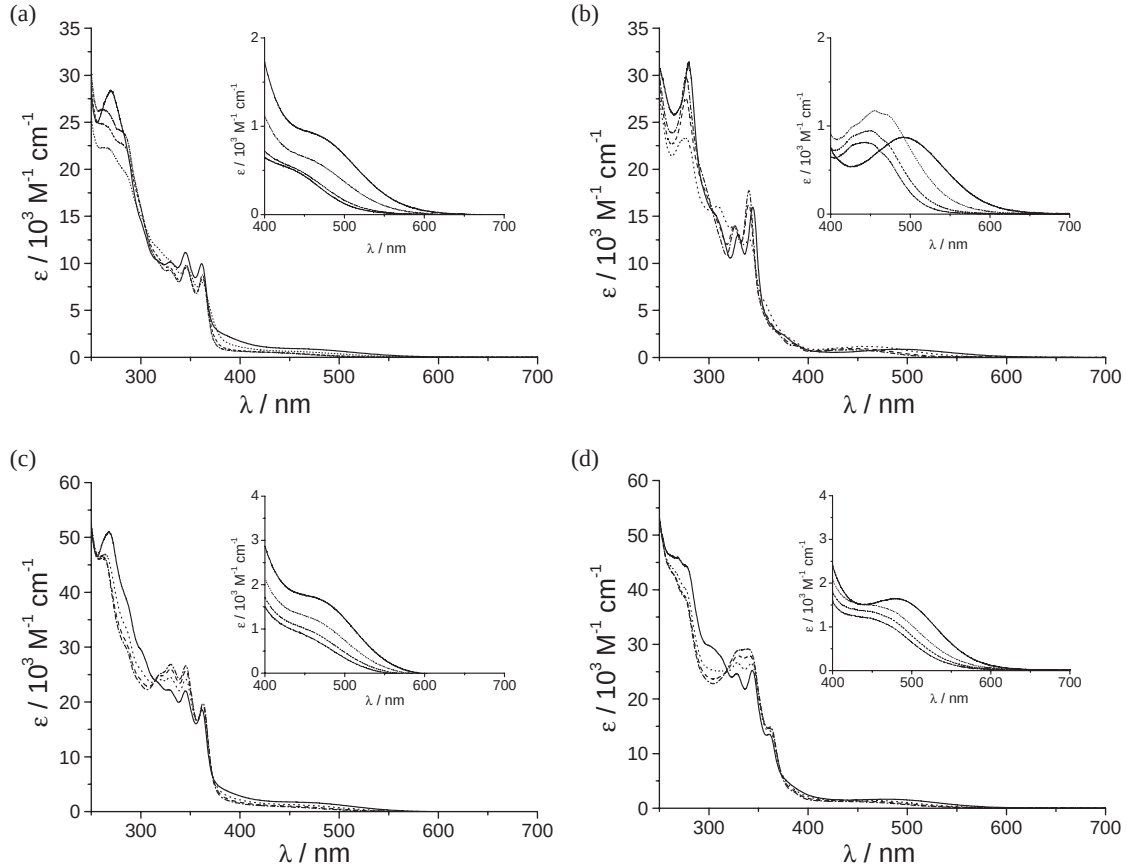

Fig. 6. UV–vis absorption spectra of the palladium and platinum complexes in acetonitrile upon addition of TsOH. (a): [**1**](PF_6), (b): [**2**](PF_6), (c): [**3**]$(PF_6)_2$, (d): [**4**]$(PF_6)_2$; solid line: without TsOH, broken line: 0.5 equiv of TsOH, dotted line: 1.0 equiv of TsOH, dashed line: 2.0 equiv of TsOH. Insets: vertical expansion of spectra at visible region.

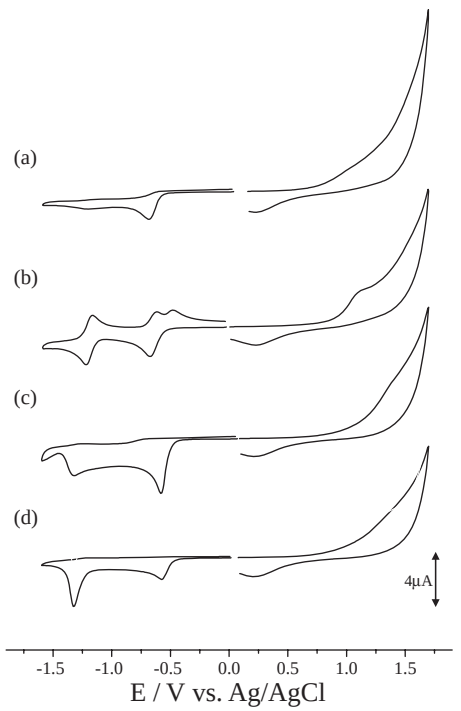

Fig. 7. Cyclic voltammograms of the complexes in DMF. (a): [**1**](PF_6), (b): [**2**](PF_6), (c): [**3**]$(PF_6)_2$, (d): [**4**]$(PF_6)_2$.

dinuclear complex $[\{Pt(terpy)\}_2(\mu\text{-dmct})]^{2+}$. Due to the highly irreversible nature of the reduction waves of the dinuclear complexes [**3**]$(PF_6)_2$ and [**4**]$(PF_6)_2$, it is not possible to determine if there is any electronic interaction between the two metal centers.

Electronic Structures of $[1]^+$ and $[2]^+$. Molecular orbital calculations were performed on the Pd(II) ($[\mathbf{1}]^+$) and Pt(II) ($[\mathbf{2}]^+$) complex cations. The energies and components of the molecular orbitals around frontier orbitals are shown in Table 3. The calculated energies and components of the MOs of the two complexes are very similar. The HOMOs of both cations are mainly composed of orbitals from the amct (>90%) and LUMOs are mainly terpy orbitals (>90%). Moreover, orbitals of the thiol groups make up 37% of the HOMOs, while those of Pd ion make up less than 5% in the HOMOs. This is consistent with the assignment of the lowest energy band as an LL(S(p) $\rightarrow$ terpy(π^*)) CT transition.[20]

Conclusion

Three palladium mercaptothiadiazole complexes have been prepared by using [Pd(OH)(terpy)](PF_6) as the starting material. In case of the platinum complexes, dmct affords both mono- and di-nuclear complexes; however, a mononuclear complex was not obtained with $\{Pd(terpy)\}^{2+}$ unit probably due to the substitution lability of palladium(II) and the solubility of the complexes. Clearly, the previous approach employing the

Table 3. Calculated Energy Levels and Components of MOs around Frontier MOs

Orbital	[1]$^+$					[2]$^+$				
	Energy /eV	Pd	S ($^-$S–R)	amct total	terpy	Energy /eV	Pt	S ($^-$S–R)	amct total	terpy
L+6	−2.93	0.00	0.00	0.00	0.99	−2.96	0.01	0.00	0.00	0.99
L+5	−3.86	0.00	0.00	0.00	1.00	−3.88	0.02	0.00	0.01	0.98
L+4	−4.47	0.01	0.00	0.00	0.99	−3.91	0.47	0.15	0.18	0.35
L+3	−4.71	0.02	0.00	0.00	0.98	−4.52	0.02	0.00	0.00	0.98
L+2	−4.85	0.47	0.17	0.19	0.34	−4.76	0.01	0.00	0.00	0.99
L+1	−5.64	0.01	0.00	0.00	0.99	−5.67	0.01	0.00	0.00	0.99
LUMO	−5.99	0.04	0.01	0.01	0.95	−6.03	0.06	0.01	0.02	0.92
HOMO	−7.86	0.03	0.37	0.95	0.02	−7.83	0.04	0.37	0.93	0.02
H−1	−9.05	0.02	0.01	0.97	0.01	−9.03	0.03	0.01	0.96	0.01
H−2	−9.27	0.06	0.30	0.92	0.02	−9.20	0.09	0.26	0.88	0.03
H−3	−9.71	0.31	0.31	0.63	0.06	−9.70	0.40	0.19	0.56	0.04
H−4	−10.21	0.04	0.05	0.95	0.02	−10.15	0.57	0.01	0.19	0.24
H−5	−10.27	0.32	0.06	0.62	0.06	−10.16	0.27	0.02	0.57	0.15
H−6	−10.44	0.32	0.00	0.03	0.65	−10.23	0.44	0.08	0.48	0.07
H−7	−10.54	0.42	0.28	0.41	0.18	−10.41	0.34	0.13	0.52	0.14

Pt(II) complexes, which has only one coordination site available for the mercaptothiadiazole ligand, is useful to prepare molecular Pd(II) complexes with mercaptothiadiazoles. Stepwise introduction of the metal center to the two thiolate groups of the dmct^{2-} enables the preparation of the platinum–palladium mixed metal dinuclear complex [{Pt(terpy)}(μ-dmct){Pd(terpy)}](PF$_6$)$_2$. The synthesis of platinum–palladium mixed metal complex indicates that dmct^{2-} symmetrically coordinates to metal ions to afford heterometallic complexes, as well as homometallic ones. The electronic spectra, cyclic voltammograms, and the MO calculation revealed the resemblance of electronic structures among the corresponding platinum and palladium complexes.

References

1 a) E. S. Raper, *Coord. Chem. Rev.* **1985**, *61*, 115. b) E. S. Raper, *Coord. Chem. Rev.* **1994**, *129*, 91. c) E. S. Raper, *Coord. Chem. Rev.* **1996**, *153*, 199. d) E. S. Raper, *Coord. Chem. Rev.* **1997**, *165*, 475. e) P. D. Akrivos, *Coord. Chem. Rev.* **2001**, *213*, 181.

2 P. Mura, B. G. Olby, S. D. Robinson, *Inorg. Chim. Acta* **1985**, *97*, 45.

3 M. V. Castaño, M. M. Plasencia, A. Macias, J. S. Casas, J. Sordo, E. E. Castellano, *J. Chem. Soc., Dalton Trans.* **1989**, 1409.

4 J. D. E. T. Wilton-Ely, A. Schier, H. Schmidbaur, *Organometallics* **2001**, *20*, 1895.

5 J. D. E. T. Wilton-Ely, A. Schier, N. W. Mitzel, H. Schmidbaur, *Inorg. Chem.* **2001**, *40*, 6266.

6 M. V. Castaño, A. Sánchez, J. S. Casas, J. Sordo, E. E. Castellano, *Inorg. Chim. Acta* **1992**, *201*, 83.

7 a) C. Ma, F. Li, D. Wang, H. Yin, *J. Organomet. Chem.* **2003**, *667*, 5. b) C. Ma, J. Zhang, F. Li, R. Zhang, *Eur. J. Inorg. Chem.* **2004**, 2775.

8 H. Tannai, K. Tsuge, Y. Sasaki, O. Hatozaki, N. Oyama, *Dalton Trans.* **2003**, 2353.

9 H. Tannai, K. Tsuge, Y. Sasaki, *Inorg. Chem.* **2005**, *44*, 5206.

10 P. Castan, F. Dahan, S. Wimmer, F. L. Wimmer, *J. Chem. Soc., Dalton Trans.* **1990**, 2679.

11 *Crystal Clear*, Rigaku Corporation, Tokyo, **1999**.

12 *teXsan v.1.11*, Molecular Structure Corporation, **2000**.

13 M. J. Frisch, G. W. Trucks, H. B. Schlegel, G. E. Scuseria, M. A. Robb, J. R. Cheeseman, J. A. Montgomery, Jr., T. Vreven, K. N. Kudin, J. C. Burant, J. M. Millam, S. S. Iyengar, J. Tomasi, V. Barone, B. Mennucci, M. Cossi, G. Scalmani, N. Rega, G. A. Petersson, H. Nakatsuji, M. Hada, M. Ehara, K. Toyota, R. Fukuda, J. Hasegawa, M. Ishida, T. Nakajima, Y. Honda, O. Kitao, H. Nakai, M. Klene, X. Li, J. E. Knox, H. P. Hratchian, J. B. Cross, V. Bakken, C. Adamo, J. Jaramillo, R. Gomperts, R. E. Stratmann, O. Yazyev, A. J. Austin, R. Cammi, C. Pomelli, J. W. Ochterski, P. Y. Ayala, K. Morokuma, G. A. Voth, P. Salvador, J. J. Dannenberg, V. G. Zakrzewski, S. Dapprich, A. D. Daniels, M. C. Strain, O. Farkas, D. K. Malick, A. D. Rabuck, K. Raghavachari, J. B. Foresman, J. V. Ortiz, Q. Cui, A. G. Baboul, S. Clifford, J. Cioslowski, B. B. Stefanov, G. Liu, A. Liashenko, P. Piskorz, I. Komaromi, R. L. Martin, D. J. Fox, T. Keith, M. A. Al-Laham, C. Y. Peng, A. Nanayakkara, M. Challacombe, P. M. W. Gill, B. Johnson, W. Chen, M. W. Wong, C. Gonzalez, J. A. Pople, *Gaussian 03, revision C.02*, Gaussian, Inc., Wallingford, CT, **2004**.

14 a) A. D. Becke, *J. Chem. Phys.* **1993**, *98*, 5648. b) A. D. Becke, *Phys. Rev. A* **1988**, *38*, 3098. c) C. Lee, W. Yang, R. G. Parr, *Phys. Rev. B* **1988**, *37*, 785.

15 a) P. J. Hay, W. R. Wadt, *J. Chem. Phys.* **1985**, *82*, 270. b) W. R. Wadt, P. J. Hay, *J. Chem. Phys.* **1985**, *82*, 284. c) P. J. Hay, W. R. Wadt, *J. Chem. Phys.* **1985**, *82*, 299.

16 a) Z. D. Bugarcic, G. Liehr, R. J. van Eldik, *J. Chem. Soc., Dalton Trans.* **2002**, 951. b) Z. D. Bugarcic, G. Liehr, R. J. van Eldik, *J. Chem. Soc., Dalton Trans.* **2002**, 2825.

17 a) S. Cosar, M. B. L. Janik, M. Flock, E. Freisinger, E. Farkas, B. J. Lippert, *J. Chem. Soc., Dalton Trans.* **1999**, 2329. b) G. M. Intille, C. E. Pfluger, W. A. Baker, Jr., *Cyrst. Struct. Commun.* **1973**, *2*, 217. c) Y. Yamada, K. Fujisawa, K. Okamoto, *Bull. Chem. Soc. Jpn.* **2000**, *73*, 2297. d) X. Liu, S. L. Renard, C. A. Kilner, M. A. Halcrow, *Inorg. Chem. Commun.* **2003**, *6*, 598. e) E. J. MacLean, R. I. Robinson, S. J. Teat, C. Wilson, S. J. Woodward, *J. Chem. Soc., Dalton Trans.* **2002**, 3518.

18 B.-C. Tzeng, A. Schier, H. Schmidbaur, *Inorg. Chem.*

1999, *38*, 3978.

19 a) B.-C. Tzeng, W.-F. Fu, C.-M. Che, H.-Y. Chao, K.-K. Cheung, S.-M. Peng, *J. Chem. Soc., Dalton Trans.* **1999**, 1017. b) M. G. Hill, J. A. Bailey, V. M. Miskowski, H. B. Gray, *Inorg. Chem.* **1996**, *35*, 4585. c) J. S. Field, R. J. Haines, D. R. McMillin, G. C. Summerton, *J. Chem. Soc., Dalton Trans.* **2002**, 1369.

20 By TD-DFT calculation, the lowest energy transitions were evaluated as the HOMO–LUMO transitions for both platinum and palladium complexes as expected. The calculated energies and oscillator strengths were 1.29 eV (960 nm) and 0.0180, and 1.34 eV (930 nm) and 0.0094, for platinum and palladium complexes, respectively. The discrepancy of the calculated and observed transition energies may be attributed to that the calculated models are ions in vacuum while the experiments are performed in the solution containing counter cations. The energies of lone pairs are relatively sensitive to the environments such as the molecular geometries, solvents, and counter ions.